

FREEZE/THAW DETECTION IN PERMAFROST REGION WITH C-BAND SCATTEROMETERS

Vahid Naeimi^(1,2), Christoph Paulik⁽²⁾, Wolfgang Wagner⁽²⁾, Annett Bartsch⁽²⁾

⁽¹⁾ *German Remote Sensing Data Center (DFD-LA), German Aerospace Center (DLR), Muenchner Strasse 20, 82234 Wessling, German, Email: vahid.naeimi@dlr.de*

⁽²⁾ *Institute of Photogrammetry and Remote Sensing, Vienna University of Technology, Gusshausstrasse 27-29, 1040 Vienna, Austria, Email: vn@ipf.tuwien.ac.at*

ABSTRACT

Distribution of permafrost is largely controlled by climatic conditions. Current permafrost monitoring methods are based on in-situ measurements and modeling and they are mostly local measurements which offer only limited insight in the impacts of global climate variations on the regional to global scale. Permafrost is a subsurface phenomenon which cannot be directly measured with remotely sensed data. But the spatial distribution, thickness and temperature of permafrost is highly dependent on the condition of the active layer overlaying the permafrost. Satellite data can be utilized for operational monitoring of the permafrost active layer by means of a number of indicators and parameters, which are highly valuable for permafrost modeling and monitoring. In this study we present the usage of backscatter measurements from ASCAT scatterometer onboard Metop for detection of freeze/thaw conditions in high latitudes and validate the results with synoptic meteorological measurements. It is shown that there is a high correlation between frozen/unfrozen flag extracted from ASCAT data and the in-situ air temperature measurements.

Key words: scatterometer, frozen ground, circumpolar

1. INTRODUCTION

The availability of high temporal resolution datasets which provide information on the freeze/thaw status of the ground is limited. LST (land surface temperature) products from MODIS or AATSR are impacted by cloud coverage and limited insolation at high latitudes [1]. Passive [2] as well as active microwave [3] satellite data are suitable for thaw and refreeze detection. Spring ground thaw coincides in general with snowmelt timing and can be thus determined using snow cover products. Fluxes do however already increase as soon as the snow starts melting [4]. Freeze-up in autumn often starts before snow covers the ground. The development of an approach for detection of snowmelt start, ground thaw and autumn freeze-up

timing is therefore required for the purpose of land-surface modelling (including permafrost) at high latitudes. This can be achieved by using microwave sensors. The suitability of Metop ASCAT for this purpose is demonstrated within this paper. The study relates to two ESA funded projects: DUE Permafrost and STSE ALANIS-Methane. The objective of the ESA DUE Permafrost (www.ipf.tuwien.ac.at/permafrost) project [5] is to establish a monitoring system for high latitude permafrost based on satellite data. Input parameters for models (numerical heat transfer, coupled atmosphere-land and dynamic vegetation models) as well as indicators at the land surface are addressed. ALANIS Methane (www.alanis-methane.info) is a research project to produce and use a suite of relevant earth observation (EO) derived information to validate and improve one of the next generation land-surface models and thus reduce current uncertainties in wetland-related CH₄ emissions [6]. It is part of ESA's Support to Science Element Program. (www.esa.int/stse). The focus on the remote sensing side of the project is the development of new and/or improved wetland maps, and snowmelt and frozen ground information [7]. Wetland dynamics are investigated on regional to local scale over Northern Eurasia for the years 2007 and 2008.

2. SCATTEROMETER DATA

Scatterometers are active microwave instruments. Spaceborne scatterometers have been originally developed for operational ocean wind monitoring but they have also been proven of high value for applications over land [8].

ASCAT (Advanced SCATterometer) onboard Metop, launched in October 2006, is a real-aperture radar operating at 5.255 GHz (C-band) with high radiometric resolution and stability. ASCAT Measurements are consistent with the preceding sensors and allow continuation of products developed for the scatterometers flown on the European Remote Sensing (ERS-1 & ERS-2) satellites [9, 10, 11]. The new instrument has the advantage of supplying information more than twice as much as the previous scatterometers

per orbit and is able to provide quasi-global data coverage over two swaths instead of one. Unlike optical instruments, ASCAT performance is unaffected by cloud cover or solar illumination and can therefore be used effectively in all-weather conditions. The long term availability of the ASCAT data together with the already existing ERS-Scatterometer dataset provide a valuable tool for long term (1991- 2020) monitoring of the Earth.

3. METHODOLOGY

Microwave backscatter differs significantly between frozen and unfrozen ground due to changing dielectric properties [12, 13, 14]. In C-band, the summer backscatter is higher than when snow is present or the ground is frozen. When the snow surfaces recrystallize after a midwinter short-term melt event, backscatter can increase up to summer levels in C-band [3]. The magnitude of the backscattered scatterometer signal is dependent on the geometric and dielectric properties of the surface. When the soil surface freezes, dielectric properties of the soil changes significantly which usually results in low backscatter values. As snow begins to fall and accumulates over the surface, due to volume scattering, backscatter signals may increase depending on microwave frequency. The response of dry snow volume to microwaves is rather complex and depends on snow properties like snow depth, density, and average grain size as well as the age of snowpack. With increasing temperature in spring, snow begins to melt and water covers the surface of snow pack which causes a sudden drop in backscatter. After the snow melting period, soil and vegetation begin to thaw and consequently backscatter arise again.

A numerical algorithm for detection of freeze/thaw conditions has been developed at the Vienna University of Technology (TU-Wien) based on the parameters and thresholds extracted by processing of the ASCAT normalized backscatter time series and using distinctive decision trees. Decisions trees are set differently with respect to the time of year. A year is divided to four main zones as depicted in fig. 3 based on seasonal Transition Points (PT1 and PT2).

In TU-Wien method, soil surface state is determined by evaluating the normalized backscatter measurement [15] at 40° incidence angle with a set of parameters, which have been calculated using two years (2007-2008) ASCAT data and comparing with modeled soil temperature data from the ECMWF ReAnalysis (ERA-Interim) dataset. The ERA-Interim dataset is based on the ECMWF Integrated Forecast Model, a global numerical weather prediction model. The resulted freeze/thaw parameter database includes seasonal transition times of year from summer to winter and vice versa (figures 1, 2), which have been calculated by

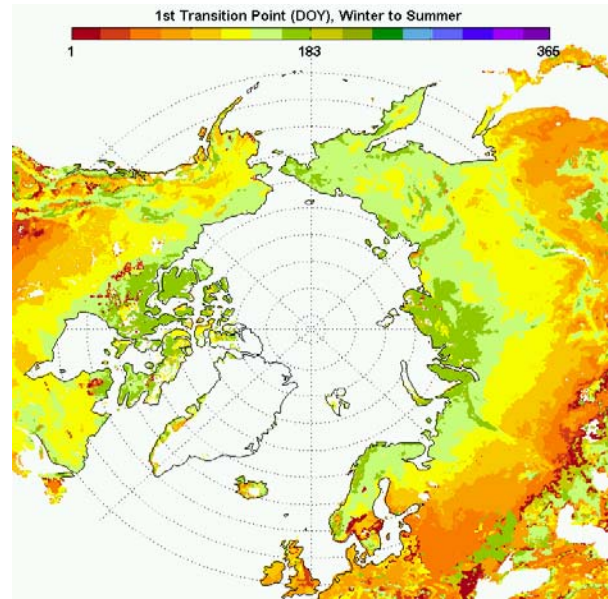


Figure 1. Seasonal transition time from summer to winter.

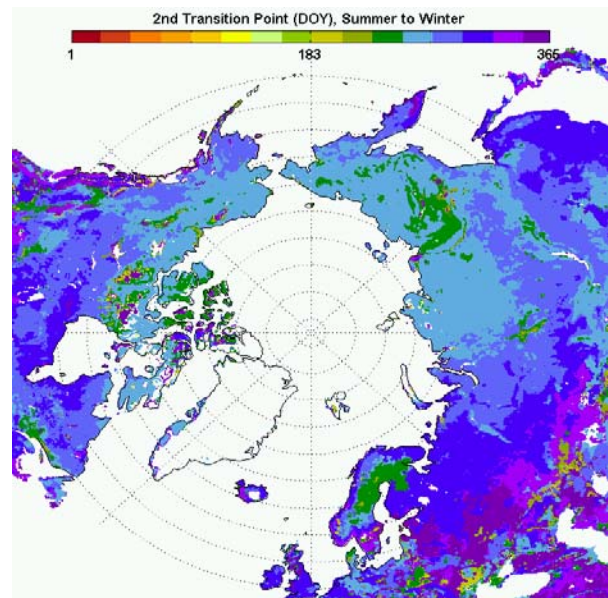


Figure 2. Seasonal transition time from winter to summer.

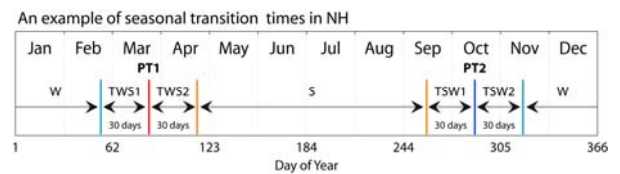


Figure 3. A year is divided to four main time periods based on Transition Points (PT): 1- Winter time, 2-First transition period (winter to summer), 3 Summer time, 4- Second transition period (from summer to winter)

implementing a step function into the time series of backscatter measurements, backscatter level during frozen conditions, and some additional statistics like the mean of backscatter in summer and winter. Fig. 4 indicates the normalized backscatter values during frozen conditions. Colors represent backscatter thresholds at frozen level in global scale and white areas indicate unknown conditions, where either the method failed to estimate the frozen level or there was not enough backscatter measurements at minus temperature to calculate the frozen level. Eventually, determination of surface state is succeeded through decision trees and by using information on normalized backscatter and freeze/thaw parameters. Fig. 5 illustrates six examples of the determined surface state for different dates.

4. RESULTS AND DISCUSSION

Comparison of the results of TU-Wien freeze/thaw detection algorithm with the air temperature data from synoptic meteorological data as well as the modeled data from Global Land Data Assimilation System (GLDAS) show significant agreement.

Fig. 6 shows a time series example of the surface state flag compared with minimum and maximum air

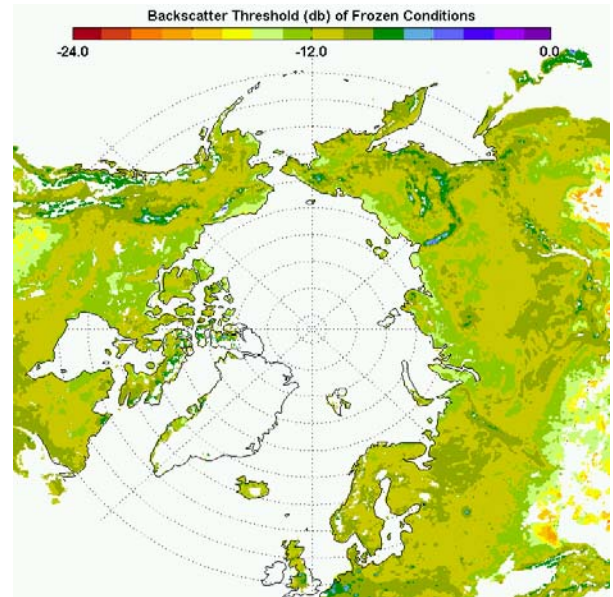


Figure 4. Backscatter level indicating threshold of frozen conditions.

temperature data from the nearest in-situ synoptic meteorological measurements.

The Calculated surface state flag indicate high correlation with air temperature measurements. The

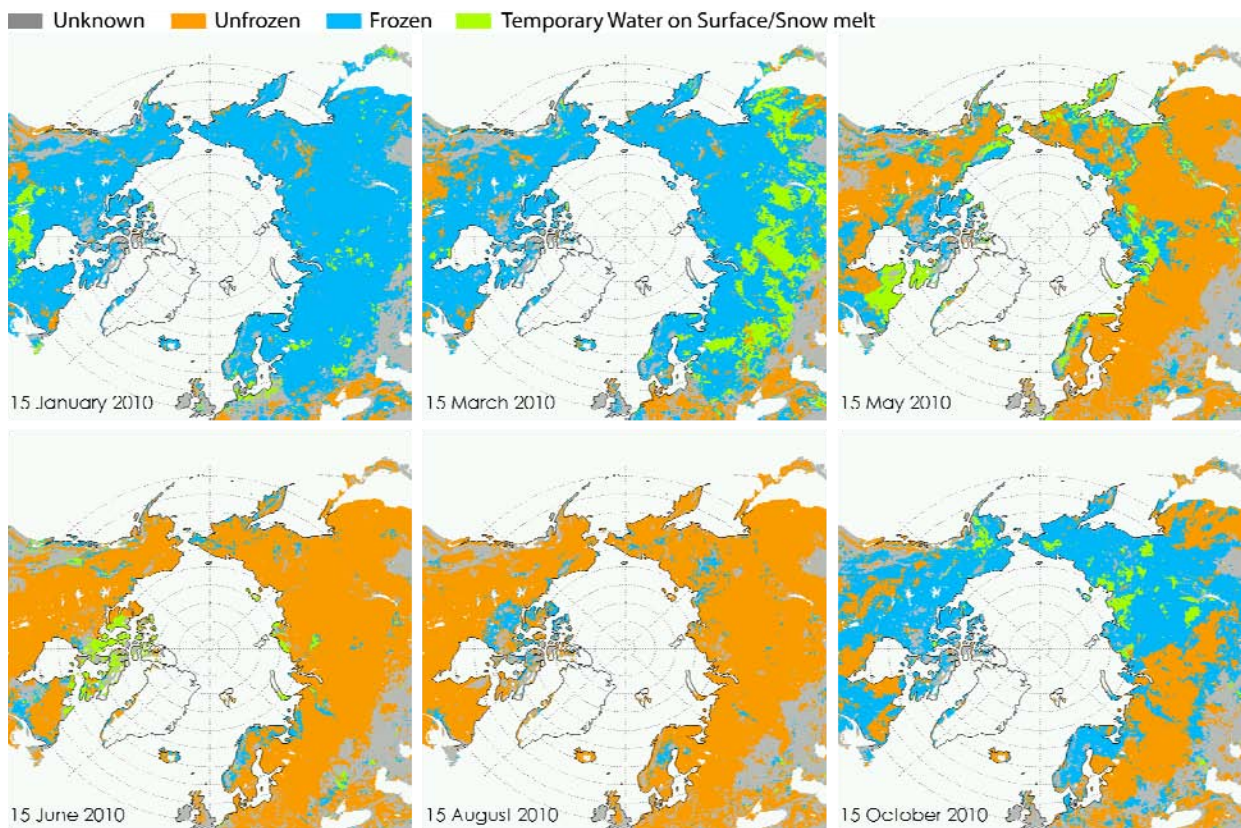


Figure 5. Estimated surface state as: frozen/unfrozen surface, temporary water on the surface or snowmelt and unknown flag.

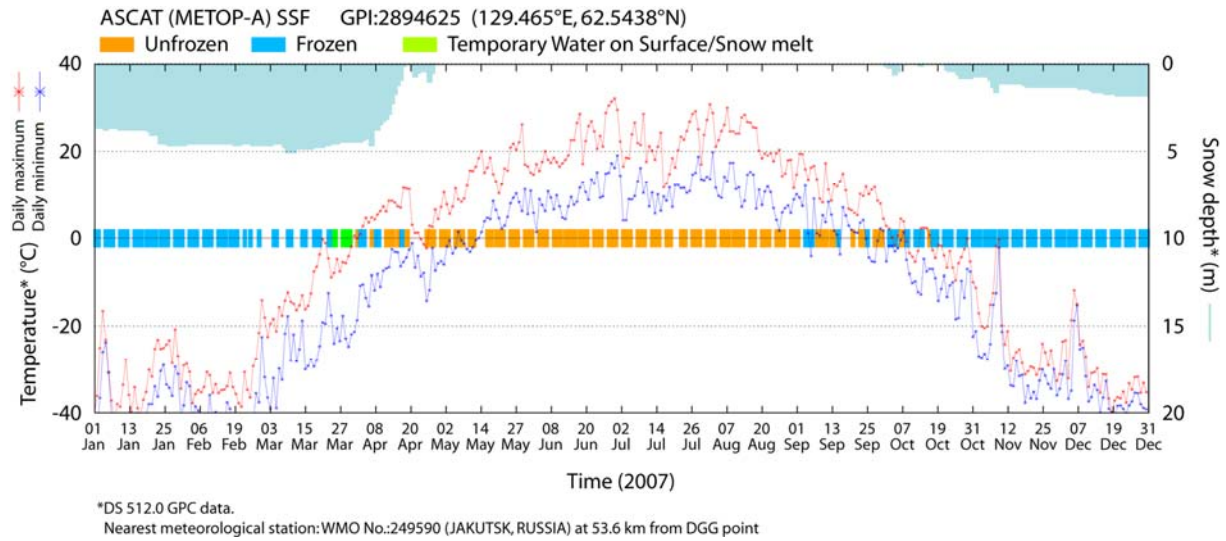


Figure 6. Time series of the estimates surface state flag compared with min/max air temperature and snow depth measurements.

agreement between the estimated surface state in this example and interpolated temperature measurements in first and second seasonal transition periods are respectively 78,8, and 85.2%. The agreement in winter and summer periods reach to respectively 98.4% and 100%.

The results of comparison between the estimated surface state flag with the GLDAS modeled temperature data in permafrost region and beyond (colored areas in fig. 4) is illustrated as in fig. 7. The most agreement is in summer and winter periods and the most distinction appears in seasonal transition periods, which are the most critical time zones for freeze/thaw detection. The existing disagreement partly comes from the uncertainties related to the estimated surface state and the modeled temperature data and partly is due to the natural difference between air and soil surface temperature.

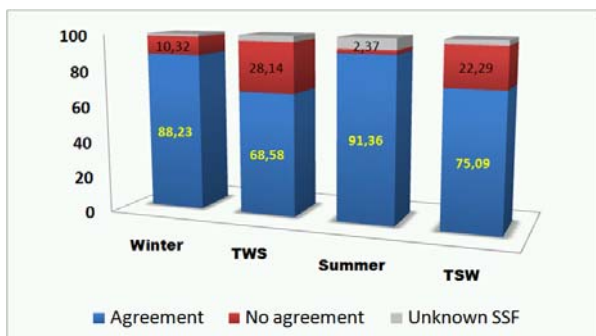


Figure 7. Comparison between the estimated surface state flag and the GLDAS modeled air temperature.

5. ACKNOWLEDGEMENTS

This study has been supported by the geoland-II project in frame of the Global Monitoring for the Environment and Security (GMES), a joint initiative of European Commission (EC) and European Space Agency (ESA), the ALANIS-methane project funded by the European Space Agency (ESA) Support to Science Element (STSE) program (ESRIN Contract No. 4000100647/10/I-LG), and the PERMAFROST project funded by the European Space Agency (ESA) Data User Element (DUE) program, which is a component of the Earth Observation Envelope Program (EOEP) (ESRIN Contract No. 22185/09/I-OL).

6. REFERENCES

- [1] A. Mialon, A. B. Royer, M. Filey, and G. Picard. Daily microwave-derived surface temperature over Canada/Alaska. *Journal of Applied Meteorology*, 46:591–604, 2007.
- [2] T. Zhang, R. L. Armstrong, and J. Smith. Investigation of the near-surface soil freeze-thaw cycle in the contiguous United States: Algorithm development and validation. *Journal of Geophysical Research*, 108:D22, 8860, 2003.
- [3] Volkmar Wismann, Monitoring of seasonal thawing in Siberia with ERS scatterometer data. *IEEE Transactions on Geoscience and Remote Sensing*, 38(4):1804–1809, 2000.
- [4] Annett Bartsch, Richard A. Kidd, Wolfgang Wagner, and Zoltan Bartalis. Temporal and spatial variability of the beginning and end of daily spring

freeze/thaw cycles derived from scatterometer data. *Remote Sensing of Environment*, 106:360–374, 2007.

[5] A. Bartsch, A. Wiesmann, T. Strozzi, C. Schmullius, S. Hese, C. Duguay, B. Heim, F. M. Seifert (2010): Implementation of a satellite data based permafrost information system *The DUE Permafrost Project. Proceedings of the ESA Living Planet Symposium*, Bergen, 2010

[6] G. Hayman, A. Bartsch, C. Prigent, F. Aires, M. Buchwitz, J. Burrows, O. Schneising, E. Blyth, D. Clark, F. O'Connor, and N. Gedney. Wetland extent and methane dynamics: An overview of the ESA ALANIS-methane project. In *ESA, iLEAPS, EGU Joint Conference on Earth Observation for Land-Atmosphere Interaction Science, 2010*.

[7] V. Naeimi, C. Paulik, W. Wagner, and A. Bartsch. Freeze/thaw detection in permafrost region with C-band scatterometers. In *ESA, iLEAPS, EGU Joint Conference: Topical Conference Earth Observation for Land-Atmosphere Interaction Science, 2010*.

[8] Wolfgang Wagner, Guenther Bloeschl, Paolo Pampaloni, Jean-Christophe Calvet, Bizzarro Bizzarri, Jean-Pierre Wigneron, and Yann Kerr. *Operational readiness of microwave remote sensing of soil moisture for hydrologic applications. Nordic Hydrology*, 38:1–20, 2007.

[9] K. D. Klaes, M. Cohen, Y. Buhler, P. Schluessel, R. Munro, J.-P. Luntama, A. V. Engeln, E. O. Clerigh, H. Bonekamp, J. Ackermann, and J. Schmetz. An introduction to the EUMETSAT polar system. *Bulletin of the American Meteorological Society*, 88(7):1085–1096, 2007.

[10] Z. Bartalis, W. Wagner, V. Naeimi, S. Hasenauer, K. Scipal, H. Bonekamp, J. Figa, and C. Anderson. Initial soil moisture retrievals from the METOP-a advanced scatterometer (ASCAT). *Geophysical Research Letters*, 34:L20401, 2007.

[11] Vahid Naeimi, Zoltan Bartalis, and Wolfgang Wagner. ASCAT soil moisture: An assessment of the data quality and consistency with the ERS scatterometer heritage. *Journal of Hydrometeorology*, 10:555–563, 2009.

[12] F. T. Ulaby, R. K. Moore, and A.K. Fung. *Microwave Remote Sensing—Active and Passive*, volume II. Artech House, Norwood, Mass., 1982.

[13] J. B. Way, R. Zimmermann, E. Rignot, K. McDonald, and R. Oren. Winter and spring thaw as observed with imaging radar at BOREAS. *Journal of Geophysical Research*, 102:29673–29684, 1997.

[14] Urs Wegmueller. The effect of freezing and thawing on the microwave signatures of bare soil. *Remote Sensing of Environment*, 33:123–135, 1990.

[15] Vahid Naeimi, Klaus Scipal, Zoltan Bartalis, Stefan Hasenauer, and Wolfgang Wagner, An Improved Soil Moisture Retrieval Algorithm for ERS and METOP Scatterometer Observations, *IEEE Transactions on Geoscience and Remote Sensing*, Vol. 47, No. 7, 2009.